Title

Numerical simulation of seawater intrusion to coastal aquifers and brine water/freshwater interaction in south coast of Laizhou Bay, China

Authors

Chang, Yawen

Hu, Bill X

Xu, Zexuan

et al.

Publication Date

2018-08-01

DOI

10.1016/j.jconhyd.2018.06.002

Peer reviewed

Numerical simulation of seawater intrusion to coastal aquifers and brine water/freshwater interaction in south coast of Laizhou Bay, China

Yawen Chang[ab] Bill X. Hu[abc] Zexuan Xu[d] Xue Li[ab] Juxiu Tong[ab] Lin Chen[ab] Hanxiong Zhang[ab] Jinjie Miao[e] Hongwei Liu[e] Zhen Ma[e]

Abstract

Seawater intrusion and brine water/freshwater interaction have significantly affected agriculture, industry and public water supply at Laizhou Bay, Shandong Province, China. In this study, a two-dimensional SEAWAT model is developed to simulate the seawater intrusion to coastal aquifers and brine water/fresh water interaction in the south of Laizhou Bay. This model is applied to predict the seawater intrusion and brine water/freshwater interface development in the coming years. The model profile is perpendicular to the coastal line with two interfaces, freshwater-saline water interface near the shore and inland brine water-saline water-seawater interface. The hydrogeological parameters in the SEAWAT-2000 model are calibrated by the head and salinity measurements. The precipitation infiltration coefficient, boundary conditions and thicknesses of aquifers are studied in a sensitivity analysis. The predicted results indicate that equivalent freshwater head in shallow freshwater-saline water area will decline 2.0 m by the end of the forecasting period, caused by groundwater over-pumping for farmland irrigation. The groundwater head in the brine-saline water area will also decrease about 1.8 m by the end of forecasting period, caused by excessive brine mining. Salinity finally decreases below 105 g/L in the brine area, but increases in other areas and contaminates fresh groundwater resources.

Keywords: Seawater intrusion, Numerical simulation, Brine water and freshwater interaction, Density dependent interface

1. Introduction

Globally, fresh groundwater resources in coastal aquifers are significantly impacted by seawater intrusion (Chang and Yeh, 2010). Climate change, sea-level rise, land use changeand groundwater overpumping have leaded to serious seawater intrusion to coastal aquifers (Yang et al., 2013; Werner et al., 2013). Coastal areas are generally the most condensed population regions in the world (Post, 2005; Sefelnasr and Sherif, 2014; Sherif et al., 2012). To meet water needs for agriculture, industry and public water supplies, groundwater resources have been seriously over exploited in the last several decades (Datta et al., 2009). The declining of groundwater level exacerbates seawater intrusion to the coastal aquifers (Ilias and Pericles, 2016), and significantly damages coastal groundwater resources (Xu et al., 2016; Lu et al., 2013; Werner and Gallagher, 2006). A harmful effect of seawater intrusion is groundwater salinization, because mixing with <1% of seawater (250 mg/L chloride) by volume makes freshwater non-potable

(Gorchev and Ozolins, 1984). According to IPCC (2007), the global average sea level will continuously rise in this century, and over-pumping groundwater resources in coastal areas are still in practice, the seawater intrusion has become a problem of worldwide concern.

Physically, seawater intrusion is a density-dependent problem (Segol et al., 1975; Segol et al., 1976; Huyakorn et al., 1987; Guo and Langevin, 2002; Langevin et al., 2003; Li et al., 2009; Hu et al., 2016; Xu and Hu, 2017). Modeling a seawater intrusion process needs to couple groundwater flow equation with solute (salt) transport equation (Priyanka and Maheshab, 2015), since the solution of salt transport is based on the groundwater flow field, which is in turn affected by salt and density distribution in the groundwater field. Many numerical models have been developed and widely applied to simulate seawater intrusion (Liu et al., 2015; Qahman and Larabi, 2004; Rajabi et al., 2015; Xu et al., 2018), including SEAWAT (Guo and Langevin, 2002; Langevin et al., 2003), SUTRA (Voss and Provost, 2002), and FEFLOW (Diersch, 2002). The solution of the coupled flow and transport equations generally requires long computational time due to the requirement of a small time step explicitly and large number of iterations in each time step implicitly (Post, 2005; Werner et al., 2013). For example, Li et al. (2009) applied a variable-density numerical code, SEAWAT 2000, to simulate a submarine groundwater discharge (SGD) caused by tidally induced sea water recirculation and a terrestrial hydraulic gradient. Owing to the computation limitation, most density-dependent numerical simulations were conducted in two-dimensional cross sections.

Most density-dependent modeling studies simulate freshwater and seawater interaction, while a few study the mixing process between freshwater and saline or brine water. Xue et al. (1997) developed a three-dimensional numerical model to simulate seawater intrusion and brine water and freshwater interaction in Longkou-Laizhou area. They studied the interface distribution between freshwater and saltwater and evolution of the transitional zone, and evaluated seawater intrusion caused by groundwater pumping. Wu et al. (1993)established a mathematical model to simulate the cation exchange between seawater and the intruded aquifer and the migration processes of Na^{+}, Ca^{2+}, Mg^{2+} in the process of seawater intrusion to the Yellow River. Yechieli et al. (2001) applied TDEM (time domain electromagnetic method) to delineate the configuration of the fresh–saline water interface in the Dead Sea coastal aquifer. Dimova et al. (2012) demonstrated that multichannel electrical resistivity can be used successfully to study fresh water and seawater interactions in volcanic coastal aquifers. Lu et al. (2013) studied steady-state freshwater-seawater mixing zone in a stratified coastal aquifer, and their results indicated that the aquifer stratification significantly affects groundwater flow and solute transport in the coastal aquifer. To characterize the shape and the evolution of the fresh water-sea water interface in a high-energy sandy beach, Buquet et al. (2015) conducted electrical resistivity tomography (ERT)

measurements from the lower beach face to the sand dune, and measured water table elevation and salinity in the dune groundwater. However, the study on brine-saline water is relatively limited. The balance law and the second law of thermo dynamics are used to obtain the groundwater motion equation in a high concentration situation (Zhang et al., 1999). Wang et al. (2003) applied PHREEQC (1997) to simulate the geochemistry evolution processes of brine water in the south coast of Laizhou Bay, China, and their results indicated that calcite, gypsum and CO_2 separated from brine during ion-exchange reactions between brine and sediment. Liu et al. (2011) analyzed the dynamic variation of underground brine water, established the correlation equation between salinity level and exploitation amount in the district and provided scientific basis for rational exploitation of brine resources. Zhang et al. (1997) studied salt-brine water intrusion and the chemical characteristics in aquifers in Weifang area, south of Laizhou Bay. Han et al. (2011) developed a mathematical model for salt/brine water intrusion to a leaky aquifer system, and described the motion of interface between salt water and fresh water in the southern beach of Laizhou Bay. Shah et al. (2013)found the carbon isotopic evidence for microbial control of carbon supply to Orca Basin at the brine-seawater interface. Saager et al. (1993) studied trace-metal distributions in seawater and anoxic brines, their results demonstrated that some metal concentrations were elevated at the seawater-brine interface and were probably associated with the presence of solid sulfide phases.

The above studies focus either on fresh water-saline water interaction area or brine-saline water area, without considering both interaction areas. In this paper, a large scale of a two-dimensional cross-section, perpendicular to the coastal line in the Laizhou bay, China is chosen to study the density-dependent mixing processes in both fresh water-saline water interface and brine-saline water interface. This study highlights that the mixing processes in both areas are interacted with each other. A numerical modeling method is developed to simulate the salinity profiles in the two zones under precipitation infiltration and groundwater pumping conditions, and to predict the variation of water quality and quantity in the south bank of Laizhou Bay in future.

2. Overview of the study area

2.1. Location and weather

The study area is located in the south of Laizhou bay, specifically in Changyi, Weifang City, Shandong Province (Fig. 1). Geographically, the area is within latitude coordinates of 36°42′~ 37°08′ and longitude coordinates of 119°21′~119°63′. The total area is about 1812 km^2. The north-south length is 75 km, and the narrowest east-west dimension is only 8 km. The coastline of the area is 35 km.

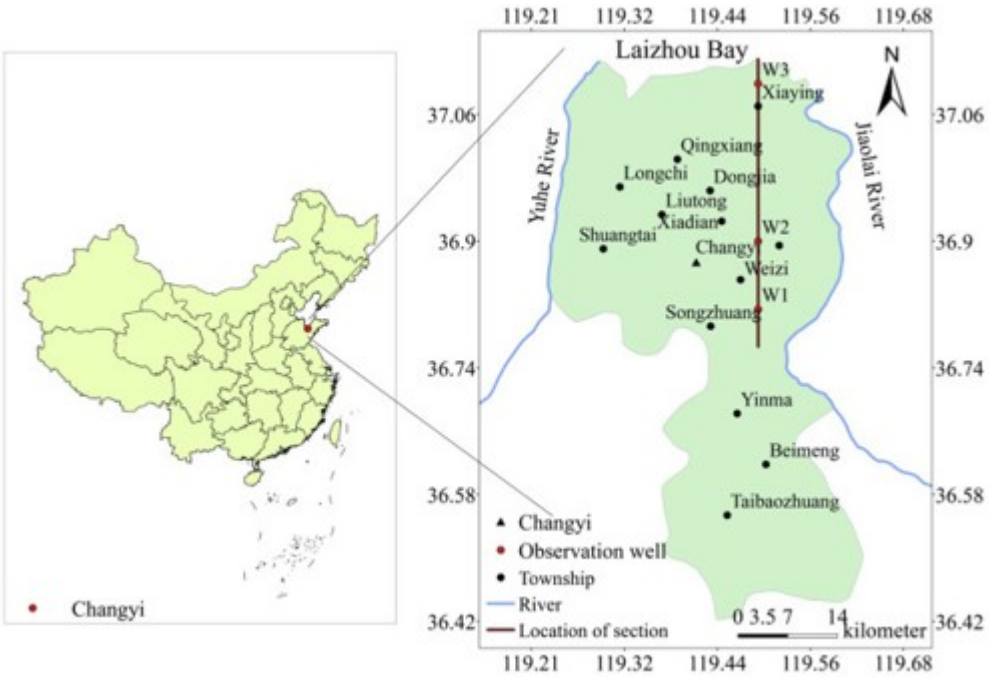

Fig. 1. Geographical location of the study area.

In the study site, the average annual precipitation from 1956 to 2012 is 612.5 mm ~ 660.1 mm, and 72.4% ~ 76.2% of the annual precipitation occurs from June to September. The evaporation (ET) from April to July is 49% of the total ET.

2.2. Geological conditions

In the study region, the coastal area in the north belongs to the alluvial plain of the Bohai depression, where Quaternary strata are widely distributed and generally thick. The coastal area is generally flat, the terrain from the south to the north declines slowly and the slope is generally <0.3‰. In the study area, the plain topography from south to north changes clearly, from alluvial plain to the sea plain.

Paleo-metamorphic rocks, Tertiary sandstones and Tertiary basalts distribute in the southern coast of the Laizhou Bay and the thickness is up to about 600 m. The strata overlying Tertiary strata are Quaternary unconsolidated sediments. The sediments are generated due to tectonic movement and changes of natural climate. The thickness of the Quaternary strata can reach 100-200 m, and the thickness becomes larger from south to north. The stratigraphy in the area from old to new is the Lower Pleistocene, the Middle Pleistocene, the Upper Pleistocene. The Upper Pleistocene is dominated by clay, and the formations are partially eroded. The Middle Pleistocene is mainly composed of coarse sand and fine sands, and the formation is thick. The Upper Pleistocene strata are the main formations in the cross-section simulated in this study. The sea-level in the area has significantly changed three times since late Pleistocene, which generated oceanic and land sediments interbedded with each other in downstream of Weihe River, and a

thick marine-terrestrial sediment layer was formed. In transgression period, many areas of the coastal plain were submerged, the seawater detained in coastal plain became brine after evaporation and concentration (Liu et al., 2016). After the marine regression, terrigenous clastic sedimentsdeposited in the coastal area, and formed very thick paleo-channel sand layers.

2.3. Hydrogeological conditions

The Quaternary alluvial to marine types loose sediments are the major aquifers widely distributed in the coastal plain area. The lithology of the water-bearing sand strata is from medium coarse sands and gravels (thickness 5–30 m) to silt, fine sands and medium sands (sand thickness 10–30 m) (Fig. 2) (modified from Zhang et al., 2017).

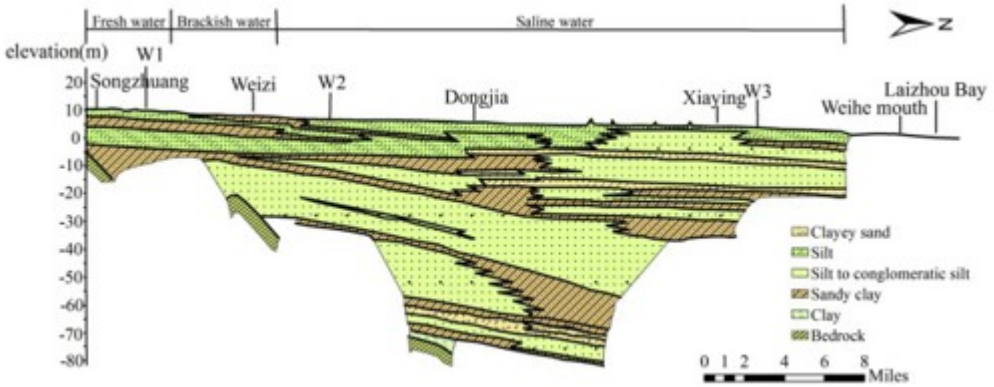

Fig. 2. Distribution of stratigraphic lithology (modified from Zhang et al., 2017).

In natural condition, the fresh groundwater subsystem in the sediment is mainly recharged by surface water, atmospheric precipitation and lateral bedrock fracture water in the southern mountainous area. The south boundary is the big, deep fault between the sediment basin and the mountain. The fault incises the entire aquifers at the south boundary of the cross section model. The river (taking a turn toward the cross-section at the fault) and piedmont fracture groundwater recharge aquifers through the fault. In the brine area, the upper layer groundwater receives recharge from precipitation, and the lower layer is supplied by brackish water and saline. Therefore, the groundwater salinity in the upper and lower layers is relative low. The groundwater salinity in the middle layers could be as high as 115,000 mg/L. The seawater had intruded the coastal aquifers in a large scale three times since the Late Pleistocene, forming the marine aquifers. After long-term evaporation and concentration, the salinity became very high in the brine aquifers.

Since the late 1970s, due to the over exploitation of fresh groundwater, the pressure difference between salt water head and freshwater head increased, and the brine water flowed through the ancient alluvial sand layer to the south quickly (Liu et al., 2004). The seawater intrusion in the study area is developed from instantaneous, small areas to continuous, large areas. There was a very broad transition zone from freshwater to saltwater in the coastal

aquifer with relatively fast intrusion speed, 11–30 km^2/year since 1984 (Xue et al., 1997). Yu and Jiaolai rivers have shallow stages, they can only be hydraulically connected with the top aquifer, but the pumping often occurs in the deeper aquifers. Further, Jiaolai river, closer to the cross-section, is about 7–8 km from the cross section, and its recharge to the the cross-section area is negligible. Only at the southern boundary of the cross section, the river could recharge aquifers since the distance from the Jiaolai river to the section is greatly reduced and a large fault exists in the southern boundary (the boundary between the mountain and the basin, in which there is a big fault in the east-west direction). In the Laizhou Bay coastal areas, shallow groundwater in the sea-land interlaced layers could be directly evaporated or receive recharge from precipitation. So the regional groundwater level is closely related with weather condition and affected by seasonal change, showing a certain periodical characteristics.

3. Groundwater flow model in the study area

3.1. Hydrological conceptual model

According to hydrogeological conditions in the section, the model area is ranged from Songzhuang Township - Weizi Town in the south to Xiaying Town -Wei River Estuary in the north. The simulation is a “pseudo” 3 dimension (3D): the total length is about 39,200 m with 1000 m extended beyond the shoreline, and the total width is 500 m. Since the width of the model is relatively small compared to the length and can be negligible, the model is in fact 2 dimension (2D). The model boundaries are defined as: according to previous studies (Gao, 2005; Han et al., 2011), the south piedmont boundary of the model is a constant flow boundary with 40 m^3/d since several small rivers and piedmont fracture groundwater recharge the aquifers; the north boundary extended into sea can be defined as a constant head and constant salt concentration boundary with 0 m and 3500 mg/L, respectively; the bottom boundary is treated as no-flow boundary; Water exchange between the aquifer and atmosphere takes place at the upper boundary, including atmospheric precipitation and evaporation. Atmospheric precipitation and evaporation during the period from January to December 2013 are measured by Changyi weather station. The precipitation recharge is estimated by the product of precipitation and precipitation infiltration coefficient of 0.15. Evaporation limit depth is 4 m. The precipitation infiltration coefficient and evaporation depth are determined from previous studies (Gao, 2005; Han et al., 2011). In the freshwater-saline water area, the pumping rate of 207,200 m^3/year is estimated according agricultural irrigationamounts for various crop requirements during the period from January to December 2013, because the pumped groundwater is mainly used for irrigation. The pumping rate divided by the area is 0.3 m^3/m^2·year, which is used in the simulation. Brine exploitation is mainly concentrated in April, May and June with a total exploitation of 486,000 m^3/a during the period from January to December 2013, which, divided by the area, is 0.43 m^3/m^2·year. Since a large number of pumping wells distribute in the actual cross section,

the pumping wells are averagely distributed in the model area and the pumping rate is the average flow rate (m^3) per unit area (m^2). In the fresh water-saline water area, pumping rates are distributed to the grids of 0-27,200 m, and in the brine-saline water area, pumping rates are distributed to the grids of 30,600–35,400 m. The lateral recharge in the piedmont is 15,330 m^3/a. The hydraulic structure of the sediment cross-section is generated according to hydraulic properties of the sediment layers. The section is divided into 15 layers. The first, third, fifth, seventh, ninth, eleventh, thirteenth, fifteenth layer are aquifers. The compositions of the aquifers are from silt to coarse gravel. The remaining layers consist of sandy clay and clay with poor permeability, and are classified as aquitards. Since the available sediment layer distribution is only part of the study region, the unavailable parts are generated according to the layer distribution patterns. The uncertainty of the generation to the simulation result is studied in Subsection 3.3.

In the freshwater-saline water area, the groundwater circulation in the south coast of Laizhou Bay is mainly controlled by precipitation, runoff and pumping processes. In recent years, due to the precipitation decrease and the over-pumping, the groundwater level declines rapidly. Since the groundwater table in coastal plain is shallow, large amount of recharge from precipitation and discharge due to evaporation are quickly processed, and the groundwater level and stored groundwater quantity have obvious seasonal and annual variation patterns.

In the brine-saline water area, the middle and deep layers in the brine funnel obtain recharge slightly from precipitation and shallow aquifers. The brine groundwater is mainly affected by the hydrostatic pressure and mining intensity in the recharge area. Its dynamic genetic type is the weak runoff - pumping type. In recent years, with the rapid development of the brine industry, brine resource was explored through the excessive pumping, resulting in continuing decline of groundwater level in the brine aquifer.

3.2. Numerical model

In this paper, a mathematical model for groundwater flow with variable density is applied to simulate the seawater and brine water intrusion processes. The numerical simulation model of solute transport in groundwater flow is established using SEAWAT-2000, which couples MT3D with MODFLOW-2000, and considers the effect of density on groundwater flow. SEAWAT-2000 has been widely applied in density-dependence flow, such as seawater intrusion (Bakker, 2003), brine mining and submarine groundwater discharge (Mao et al., 2006; Li et al., 2009).

3.2.1. Governing equation

The governing equation for the variable density groundwater flow in the study area can be expressed as (1):

$$\frac{\partial}{\partial x}\left(\rho K_{fx}\left[\frac{\partial h_f}{\partial x}+\left(\frac{\rho-\rho_f}{\rho_f}\right)\frac{\partial Z}{\partial x}\right]\right)+\frac{\partial}{\partial y}\left(\rho K_{fy}\left[\frac{\partial h_f}{\partial y}+\left(\frac{\rho-\rho_f}{\rho_f}\right)\frac{\partial Z}{\partial y}\right]\right)$$
$$+\frac{\partial}{\partial z}\left(\rho K_{fz}\left[\frac{\partial h_f}{\partial z}+\left(\frac{\rho-\rho_f}{\rho_f}\right)\frac{\partial Z}{\partial z}\right]\right)=\rho S_f\frac{\partial h}{\partial t}+\theta\frac{\partial \rho}{\partial C}\frac{\partial C}{\partial t}-\overline{\rho}_s q_s \quad (1)$$

where h_f is the equivalent fresh water head [m]; ρ_f is the density of fresh water [kg/m^3]; q_s is unit volume flow of the source (sink) [1/s]; θ is the effective porosity of porous medium; S_f is the unit water storage coefficient of equivalent fresh water [1/m]; K_{fs} is the permeability coefficient of equivalent freshwater [m/s].

The equation of solute transport is expressed as,

$$\frac{\partial(\theta C^k)}{\partial t}=\frac{\partial}{\partial x_i}\left(\theta D_{ij}\frac{\partial C^k}{\partial x_i}\right)-\frac{\partial}{\partial x}\left(\theta\vartheta_i C^k\right)+q_s C_k^s+R_n \quad (2)$$

where C_k is the dissolved concentration of substance k [mg/L]; D_{ij} is the hydrodynamicdispersion coefficient [m^2/s]; C_k^s is concentration of substance k in source or sink term [mg/L]; R_n is reaction term of chemical substance.

3.2.2. Model domain discretization

This model domain is discretized into rectangular grids with $500 \times 100 \times 500\ m^3$. There are 392 columns and 15 layers with 5880 cells in total. The simulation period is from January 1, 2013 to December 31, 2013, and each month is taken as a stress period, and the number of days in a stress period is used as a time step.

3.2.3. Model calibration

The empirical values of vertical hydraulic conductivity, specific yield, specific storage, effective porosity of the corresponding lithology (Wang et al., 1995) are used for the initial values of the parameters. The horizontal conductivity is assumed to be 10 times of its vertical value. The parameters of aquifers are calibrated by trial-error method repeatedly to fit the head and salinity measurements. The process of calibration is to adjust the values of several parameters, such as hydraulic conductivity, specific yield, specific storage, effective porosity, until the mean error (ME) between the observed values and the calculated values at the three observation wells (W1, W2, W3) are <10% of the maximum observed value variations. The locations of observation wells (W1, W2, W3) are labeled in Fig. 1. The observation depths of W1, W2, W3 are respectively, 5.4 m, 40.1 m, 41.3 m.

Fig. 3 shows the observed values and the calculated values of hydraulic heads and salt concentrations at the end of simulation period. The ME values between observed and calculated heads at W1, W2, W3 are −0.002 m, 0.007 m, 0.003 m, respectively, and root-mean-square error (RMSE) are

0.039 m,0.012 m, 0.005 m, respectively. The ME values between observed and calculated concentrations at W1, W2, W3 are −0.146 mg/L, 0.009 mg/L, 1.267 mg/L, and RMSE values are 0.273 mg/L, 0.025 mg/L, 4.016 mg/L, respectively. These errors are small relative to the maximum head variations of ~0.26 m, ~0.19 m and ~0.18 m in the three observed wells, and small relative to the maximum concentration variations of ~4 mg/L, ~0.32 mg/L and ~100 mg/L in the wells. The results indicate that the errors have been minimized. In general, the simulated groundwater levels and salt concentrations match the observations well.

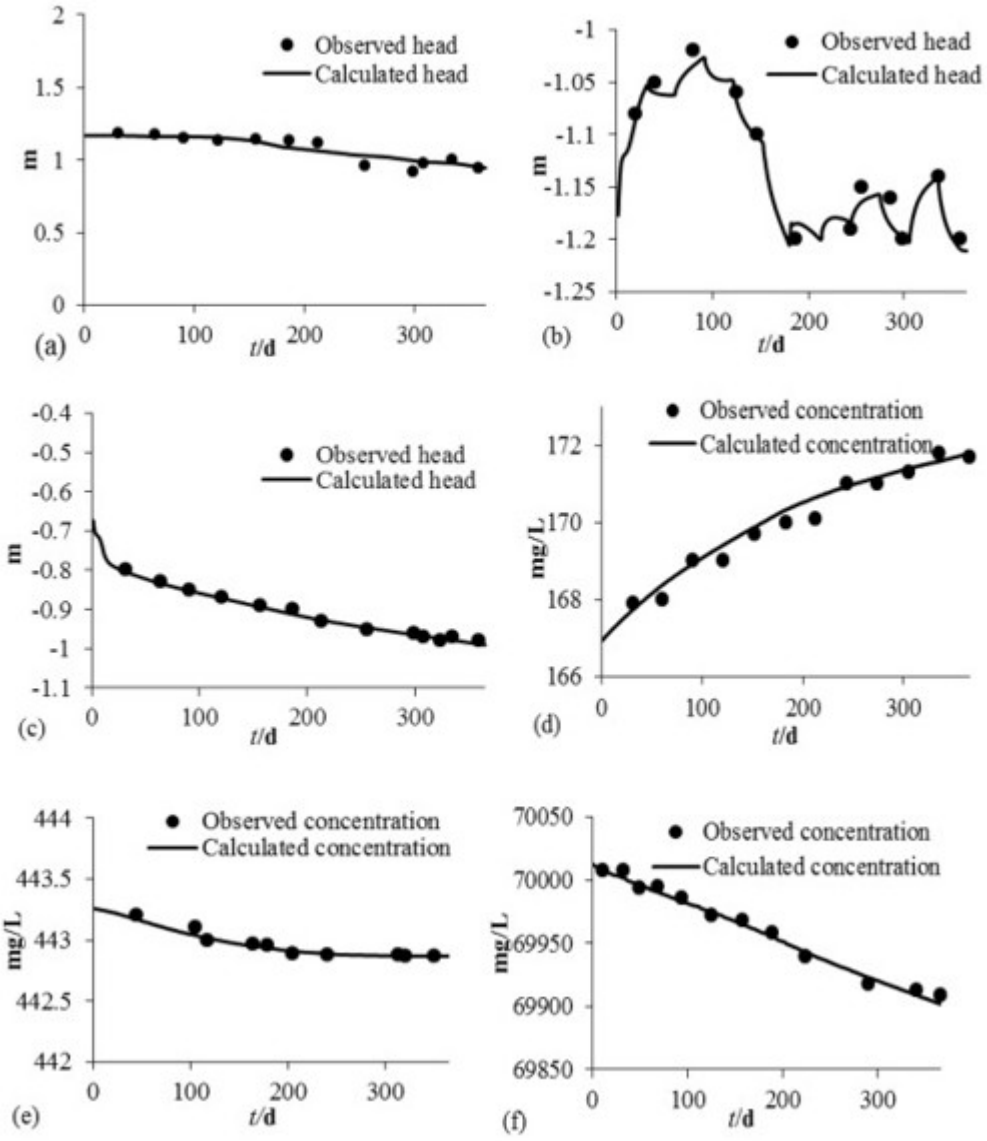

Fig. 3. Fitting of observed values and calculated values of hydraulic head and concentration (a) hydraulic head at W1; (b) hydraulic head at W2; (c) hydraulic head at W3; (d) salinity at W1; (e) salinity at W2; (f) salinity at W3.

3.3. Sensitivity study

3.3.1. Calibrated parameters and numerical simulation results

According to the lithology, the calibrated vertical hydraulic conductivity, specific yield, specific storage and effective porosity are shown in Fig. 4. Based on empirical data, the horizontal hydraulic conductivity value is assumed to be ten times of the vertical hydraulic conductivity value. The first and the third layers are mainly consisted of coarse sands with larger hydraulic conductivity values. In addition, the remaining parameters in the model are not calibrated. Longitudinal dispersivity and transversal dispersivity are 500 m and 50 m respectively, and diffusion coefficient is 8.64×10^{-5} m^2/d.

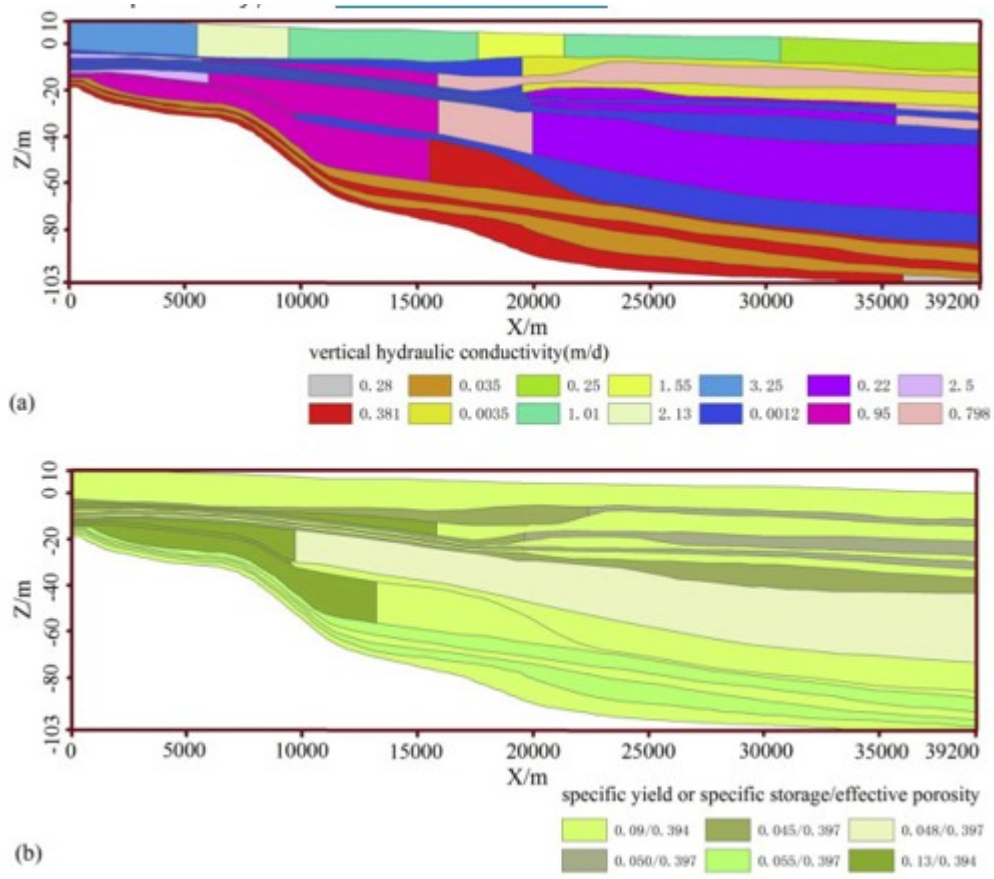

Fig. 4. Model parameter (a) vertical hydraulic conductivity (m/d); (b) specific yield or specific storage and effective porosity.

The groundwater flow field (Fig. 5) and concentration field (Fig. 6) could well describe the groundwater level and salinity distributions in the study area, in which there are freshwater-saline area and brine-saline water area. In freshwater-saline area, the groundwater head is relatively high, basically >0 m, and salinity is <20,000 mg/L. Pumping groundwater occurs in shallow aquifers and the pumped water is used for irrigation. In brine-saline water area, there is a depression cone with a depth of 7.0 m below sea level, and its salinity is about 100,000 mg/L. The brine exists in the deep aquifer, and

the brine water is pumped for salt industry, which has been practiced for several decades.

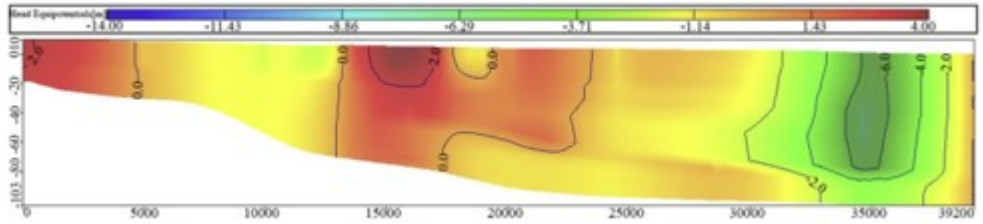

Fig. 5. Groundwater flow field at the end of simulation.

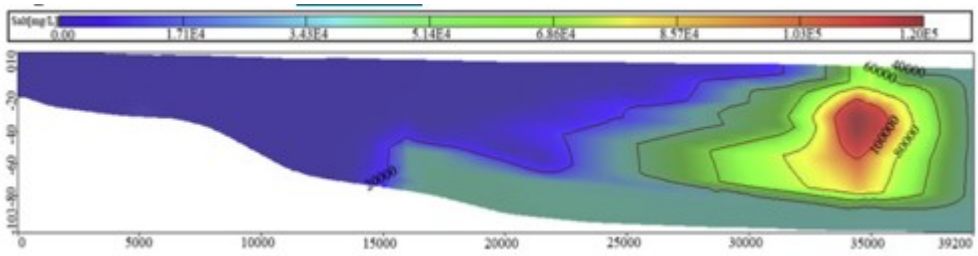

Fig. 6. Groundwater salinity field at the end of simulation.

3.3.2. Hydrogeological structure and parameter uncertainty analysis

Natural media are generally heterogeneous. In the practical application, the adjacent aquifers with similar lithology are often combined to be one. The aquifer distributions (Fig. 4) are mainly based on the available distribution of stratigraphic lithology in the study area shown in Fig. 2 (modified from Zhang et al., 2017). In order to examine the influence of thickness variations of aquifers on the simulation results, two representative layers, the first and the third layers of the media, are selected to conduct the sensitivity analysis. The reason to choose the two layers is that the permeability values of the two layers are relatively high, and their thickness variations can have greater impact on groundwater flow and salt transport simulation than other layers. The thicknesses of the selected two layers were increased by 15% or decreased by 15%. The simulation results indicate that the variations of the layer thicknesses slightly affect the simulation results.

Precipitation infiltration coefficient with 0.15 is obtained by referring previous studies (Gao, 2005). In the sensitivity study, the precipitation infiltration coefficient was set to 0.1 or 0.2. The results also indicate that the variations of the infiltration coefficient slightly affect the simulation results.

The boundary flow amount is obtained from previous study (Gao, 2005). The southern boundary is located at the junction of the plain area and the hill area, and its sources of recharge are the lateral outflow from the piedmont area and the base flow from the hill area. The lateral outflow is 2,088,300 m^3/a, recharging groundwater in the plain area. River base flow is 8,226,900 m^3/a, recharging groundwater through river seepage to the fault. According to the model width's proportion of the entire flow section, the southern boundary flow is 40 m^3/d. The boundary flow was increased by 15% or

decreased by 15% in the sensitivity study. The results indicate that the variations of the boundary flow slightly affect the simulation results in the freshwater/salty water and brine water/seawater regions.

Since the north boundary is extended 1000 m beyond the shoreline, the boundary influence on the simulation result was trivial, so the boundary is reasonably defined as a constant head, 0.0 m. Since the tide fluctuations are not considered, so we only conduct sensitivity study on the constant head variation. The value of constant head was set to -1 m or 1 m, which is close to the water head of low tide or high tide in the south coast of Laizhou Bay. The simulation results indicate that the variations of the constant head slightly affect the simulation results, so the modeling result is not very sensitivity to the variations of the constant head boundary.

4. Prediction results and analysis

The model calibration results indicate the developed model is reasonably calibrated and could be used for prediction. The prediction simulation period for groundwater flow and solute transport in the cross-section area is 7 years (from January 2014 to December 2020). Numerically, the simulation period was divided into 84 monthly stress periods in total. The groundwater flow and salt concentration fields at January 2014 are chosen as initial conditions. Hydrogeological parameters used are recognized and verified. The sink and source terms during the predict periods are specified as: the rainfall has the periodicity, and the rainfall period during the period from January 1983 to December 1989 is a rainfall cycle, and assumed to be the cycle for the period from January 2014 to December 2020 in the prediction model. In the seven years, there are three consecutive dry years (>75% cumulative frequency, rainfall < 483.1 mm), which can allow our model to meet the requirements for predicting groundwater level and quality trends under special climate conditions. Also, the evaporations from 1983 to 1989 are taken as the evaporation inputs in the prediction simulation. Pumping rates from 2014 to 2020 are taken as the same as those in 2013 in the freshwater-saline water area and brine-saline water area.

The simulated hydraulic heads during the simulation period at the position ($X = 4949$ m, $Z = -6$ m) are shown in Fig. 7(a). From the figure, groundwater declines with time in the shallow freshwater area. In a hydrological year, the amount of groundwater pumping would increase with less precipitation and more evaporation when spring irrigation season starts. Therefore, the water level declines 0.3 m to the lowest in June. Then, the groundwater table will rise slowly with the precipitation increase and groundwater exploitation decrease, and reach the highest level in September or October. Due to large water demand for winter wheat, the water level declines from November to February in the following year. For many years, the groundwater level will decrease year by year due to the continuous drought condition, the reduction of the precipitation recharge and the excessive exploitation of groundwater. A large hydraulic cone has formed in the coastal plain, induced

seawater intrusion to the freshwater aquifer. As shown in Fig. 7(b), the salinity of the shallow freshwater area increases, the main reason is that the exploitation amount of fresh water is higher than recharge, which decreases hydraulic head and increases salt water inflow into the shallow layers.

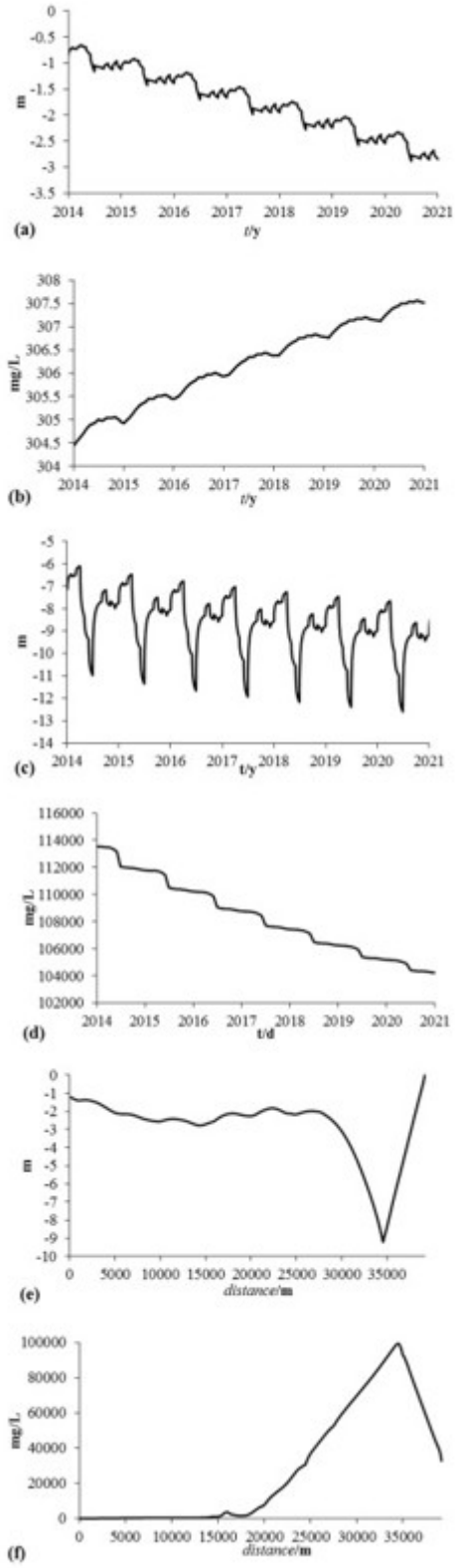

Fig. 7. Variation of (a) groundwater head and (b) salinity with time in the shallow fresh water area ($X = 4949$ m, $Z = -6$ m) affected by the pumping. Variation of (c) groundwater head and (d) salinity

with time in the brine funnel affected by the pumping. (e) Groundwater head and (f) salinity varies with distance in December 2020.

In the deep layers of the funnel area, the depth of the deepwater recharge zone is large, and the hydraulic head is slow to restore, the water level has been decreasing for many years, as shown in Fig. 7(c). In the forecast periods, the annual variation is about 6 m, and the mean hydraulic head decreases about 1.8 m in the next 7 years. The hydraulic gradient in the northern brine zone will increase, which would increase seawater intrusion to the groundwater. As shown in Fig. 7(d), the salinity of the deep brine funnel is also decreased, mainly due to the pumping of the brine with high salinity, while the recharge of freshwater or seawater with relatively low salinity will dilute the brine water salinity.

The distributions of groundwater head and salt concentration in December 2020 are taken for analysis. The area is mainly in a sandy aquifer with a thickness of 10 to 30 m. The burial depth of aquifers increases from the piedmont to Laizhou Bay. It can be seen from Fig. 7(e) that the groundwater head is that high-low-slightly high-extremely low-high from the piedmont to Laizhou Bay. The low-level in freshwater-saline area is the concentrated freshwater exploration area. The distribution of pumping wells is not uniformly distributed in the farmlands, with large variation of annual pumping amounts over the years. A number of small depression cones are formed in this area. The second extremely low water level area is brine-saline water area, and it is also located in the brine depression cone area. The water levels are slightly higher between the depression cones, because groundwater salinity in this area does not meet the standards of irrigation and domestic use, also does not satisfy the requirements for salt production, so the pumping rate is low. Due to soil salinization, farmlands in this area are abandoned or the yield is very low. Fig. 7(f) shows the variation of groundwater salinity from the hillslope to the coastal area. Aquifer salinity is the highest in the depth of 30 m–40 m, mainly due to the existence of ancient sedimentary brine in this layer.

In the simulated area, the change of hydraulic head is obvious within a year, and hydraulic head declines to the lowest in June, particularly in the brine area. In spring, the weather is relatively dry and the evaporation is large, and in addition, a lot of brine is pumped for salt industry. After June, the water level will recover gradually and in December the water level is relatively high. Although the water level changes during the year, the overall trend has been declining year by year.

Fig. 8 shows that horizontally freshwater is dominant in the inland, and high mineralized water is dominant in coastal areas. In the last several decades, the salinity around in the brine area has gradually decreased, mainly due to the brine exploitation. Reduction of the brine salinity is irreversible, because brine is formed during seawater intrusions in a geological time period and under special geological conditions. However, the salinity of 20,000 mg/L in the center of brine area does not change significantly with time, because the

center is located between fresh water-saline water area and brine-saline water area, affected by the pumping in both areas, and the pumping effects from both side are similar.

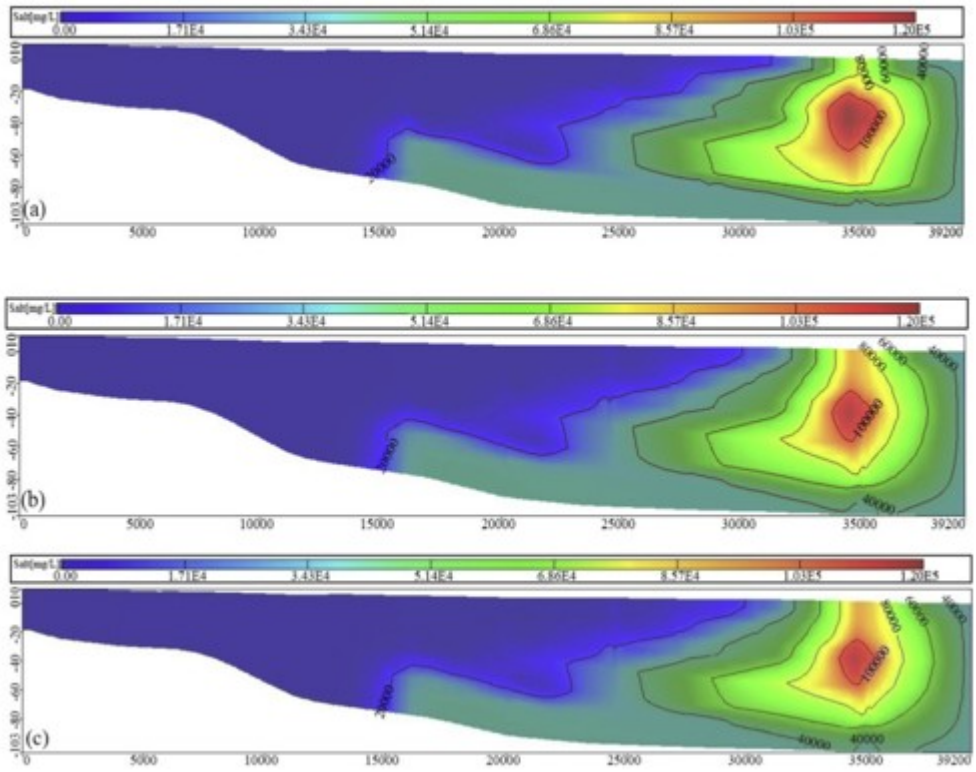

Fig. 8. Distribution of groundwater salinity in (a) December 2014; (b)December 2019; (c) December 2020.

5. Summary and conclusions

Based on previous field study (Ma et al., 1997; Xue et al., 1997; Han et al., 2001), a two-dimensional density-dependent SEWAT model is established to predict the seawater intrusion and brine water/salty water interaction in coastal aquifers in a cross-section perpendicular to South Coast of Laizhou Bay (Shandong Province, China). There are two major hydraulic cones along the cross-section that interact with each other, one is caused by fresh groundwater pumping for agriculture production and another is due to the brine pumping for salt production. Two major interfaces, including freshwater/saline water and saline water/seawater, are numerically simulated in this study. Based on the measured data from January 1, 2013 to December 31, 2013, the model is calibrated by a trial-and-error method. The model parameters are calibrated by head and salinity observations. The calibrated model is used to predict the trend of seawater intrusion under various mining conditions. Based on the study results, the following conclusions are made.

1.

Based on the sensitivity study on precipitation infiltration coefficient, boundary conditions, aquifer thickness uncertainty, the variations of the above factors would slightly affect the simulated results for flow and salt transport in the study area. The results indicate that the estimated distributions of hydraulic conductivity and porosity, based on the incomplete distribution of stratigraphic lithology in the study area, are reasonable, and the simulation results based on the distributions are reliable.

2.

The hydraulic head fluctuates and decreases along the whole profile. The prediction results indicate hydraulic head at the freshwater-saline water area decreases during the drought years with 0.3 m annual variation, and declines 2 m in total by the end of the simulation period. The hydraulic head in the brine mining area is also decreasing year by year, and the annual variation is about 6 m, and the hydraulic head decrease in forecasting period is about 1.8 m. A larger depression cone appears in the brine zone, and several smaller depression cones in other areas. The salinity of the brine decreases gradually and finally drops below 105 g/L and the salinity of the other areas increases.

3.

The study results indicate the current groundwater explorations in freshwater and brine areas are not sustainable. The overpumping in the brine area will significantly decrease the brine salinity, indicating the less effective production and high cost of brine production in this area. The overpumping in the fresh water area will increase water and soil salinity, significantly damage groundwater quality and reduce fresh groundwater resources.

Acknowledgements

This work was partly supported National Natural Science Foundation of China (41530316) and National Key Research Project (2016YFC0402805).

References

Bakker, 2003

M. Bakker**A Dupuit formulation for modeling seawater intrusion in regional aquifer system**

Water Resour. Res., 39 (5) (2003), p. 1131

Buquet et al., 2015

D. Buquet, C. Sirieix, P. Anschutz, P. Malaurenta, C. Charbonnierb, F. Naessensa, S. Bujanb, P. Lecroartb**Shape of the shallow aquifer at the fresh water-sea water interface on a high-energy sandy beach**

Estuar. Coast. Shelf, 179 (2015), pp. 79-89

Chang and Yeh, 2010

C.M. Chang, H.D. Yeh**Spectral approach to seawater intrusion in heterogeneous coastal aquifers**

Hydrol. Earth Syst. Sci., 14 (5) (2010), pp. 719-727

Charlton et al., 1997

S.R. Charlton, C.L. Macklin, D.L. Parkhurst**PHREEQCI—a graphical user interface for the geochemical computer program PHREEQC**

U.S. Geological Survey Water-Resources Investigations Report 97-4222 (1997)

Datta et al., 2009

B. Datta, H. Vennalakanti, A. Dhar**Modeling and control of saltwater intrusion in a coastal aquifer of Andhra Pradesh, India**

J. Hydro Environ. Res., 3 (2009), pp. 148-159

Diersch, 2002

H.J.G. Diersch**WASY Software-FEFLOW: Finite Element Subsurface Flow & Transport Simulation System**

WASY, Berlin (2002)

Dimova et al., 2012

N.T. Dimova, P.W. Swarzenski, D. Henrieta, C.R. Glenn**Utilizing multichannel electrical resistivity methods to examine the dynamics of the fresh water-seawater interface in two Hawaiian groundwater systems**

J. Geophys. Res., 117 (C2) (2012), p. 2012

Gao, 2005

S.D. Gao**The Estimation of the Groundwater Resources in Weifang City**

(Master)

Hohai University, Nanjing (2005)

Gorchev and Ozolins, 1984

H.G. Gorchev, G. Ozolins**WHO guidelines for drinking-water quality**

Who Chron., 38 (3) (1984), p. 104

Guo and Langevin, 2002

W. Guo, C.D. Langevin**User's guide to SEAWAT: a computer program for simulation of three-dimensional variable-density groundwater flow**

US Geol. Surv. (2002), pp. 1-434

Han et al., 2001

Han, F., Xue, Y.Q., Wu, J.C., Ye, S.J., 2001. Hydrochemical characteristics of groundwater in salt-water intrusion condition and genesis of brine along the south coast of the Laizhou Bay, China. Geol. Rev. 47 (1), 102–108.

Han et al., 2011

F. Han, J.C. Wu, Y.X. Zhang**Numerical simulation for the salt/brine water intrusion in a leaky aquifer: a case study of the southern beach of Laizhou Bay, eastern China**

J. Nanjing Univ., 47 (3) (2011), pp. 281-290

Hu et al., 2016

B.X. Hu, Y. Cao, W. Zhao, F. Bao**Identification of hydraulic conductivity distributions in density dependent flow fields of submarine groundwater discharge modeling**

Chin. Sci. Earth Sci., 59 (1) (2016), pp. 1-10

Huyakorn et al., 1987

P.S. Huyakorn, P.F. Anderson, J.W. Mercer, H.O. White**Saltwater intrusion in aquifers: development and testing of a three dimensional finite element model**

Water Resour. Res., 23 (2) (1987), pp. 293-321

Ilias and Pericles, 2016

S. Ilias, L. Pericles**Modeling seawater intrusion in overexploited aquifers in the absence of sufficient data: application to the aquifer of NeaMoudania, northern Greece**

Hydrogeol. J., 24 (8) (2016), pp. 2123-2141

Langevin et al., 2003

C.D. Langevin, W.B. Shoemaker, W. Guo**MODFLOW-2000, the U.S. Geological Survey modular ground-water model: documentation of the SEAWAT-2000 version with variable density flow process (VDF) and the integrated MT3DMS transport process (IMT)**

US Geol. Surv. (2003), pp. 3-426

Li et al., 2009

X.Y. Li, X.H. Bill, W.C. Burnett, I.R. Santos, J.P. Chanton**Subarine groundwater discharge driven by tidal pumping in a heterogeneous aquifer**

Ground Water, 47 (4) (2009), pp. 558-568

Liu et al., 2004

E.F. Liu, Z.L. Zhang, J. Shen, J.F. Song**Origin and characteristics of salt-water intrusion disaster in the downstream of Weihe River on the south coast of Laizhou Bay**

J. Earth Sci. Environ., 26 (3) (2004), pp. 78-82

Liu et al., 2011

G. Liu, X.J. Han, S.T. Feng, Q.A. Tian**Study on relation between dynamic change and water exploitation amount of underground brine water in south coast of Laizhou Bay**

Territ. Resour. Shandong Province, 27 (2011), pp. 12-15

Liu et al., 2015

Y. Liu, X. Mao, J. Chen, D.A. Barry**Influence of a coarse interlayer on seawater intrusion and contaminant migration in coastal aquifers**

Hydrol. Process., 28 (20) (2015), pp. 5162-5175

Liu et al., 2016

Y. Liu, J.J. Jiao, X. Luo**Effects of inland water level oscillation on groundwater dynamics and land-sourced solute transport in a coastal aquifer**

Coast. Eng., 114 (2016), pp. 347-360

Lu et al., 2013

W. Lu, Q. Yang, J.D. Martin, R. Juncosa**Numerical modeling of seawater intrusion in Shenzhen (China) using a 3D density dependent model including tidal effects**

J. Hydro Environ. Res., 122 (2) (2013), pp. 451-465

Ma et al., 1997

F.S. Ma, Z.H. Cai, W.H. Song**Saline intrusion mechanism and its control measures**

Chin. J. Geol. Hazard Control, 8 (4) (1997), pp. 18-22

Mao et al., 2006

X. Mao, P. Enot, D.A. Barry, L. Li, A. Binleye, D.-S. Jengf**Tidal influence on behavior of a coastal aquifer adjacent to a low-relief estuary**

J. Hydrol., 327 (1–2) (2006), pp. 110-127

Post, 2005

V.E.A. Post**Fresh and saline groundwater interaction in coastal aquifers: is our technology ready for the problems ahead**

Hydrogeol. J., 13 (1) (2005), pp. 120-123

Priyanka and Maheshab, 2015

B.N. Priyanka, A. Maheshab**Parametric studies on saltwater intrusion into coastal aquifers for anticipate sea level rise**

Aquat. Procedia, 4 (2015), pp. 103-108

Qahman and Larabi, 2004

K. Qahman, A. Larabi**Numerical modeling of seawater intrusion in Khan-Younis area of the Gaza Strip Aquifer, Palestine**

Dev. Water Sci., 55 (4) (2004), pp. 1629-1641

Rajabi et al., 2015

M.M. Rajabi, B. Ataie-Ashtiani, C.T. Simmons**Polynomial chaos expansions for uncertainty propagation and moment independent sensitivity analysis of seawater intrusion simulations**

J. Hydrol., 520 (1) (2015), pp. 101-122

Saager et al., 1993

P.M. Saager, J. Schijf, H.J.W.D. Baar**Trace-metal distributions in seawater and anoxic brines in the eastern Mediterranean Sea**

Geochim. Cosmochim. Ac., 57 (7) (1993), pp. 1419-1432

Sefelnasr and Sherif, 2014

A. Sefelnasr, M. Sherif**Impacts of seawater rise on seawater intrusion in the Nile Delta aquifer**

Egypt. Ground Water, 52 (2) (2014), pp. 264-276

Segol et al., 1975

G. Segol, G.F. Pinder, W.G. Gray**A Gelarkin finite element technique for calculating the transient position of saltwater front**

Water Resour. Res., 11 (2) (1975), pp. 343-347

Segol et al., 1976

G. Segol, G.F. Pinder, W.G. Gray**Transient simulation of saltwater intrusion in Southeast Florida**

Water Resour. Res., 12 (1) (1976), pp. 65-70

Shah et al., 2013

S.R. Shah, S.B. Joye, J.A. Brandes, A.P. Mcnichol**Carbon isotopic evidence for microbial control of carbon supply to Orca Basin at the brine-seawater interface**

Biogeosciences, 10 (5) (2013), pp. 3175-3183

Sherif et al., 2012

M. Sherif, A. Sefelnasr, A. Javadi**Incorporating the concept of equivalent freshwater head in successive horizontal simulations of seawater intrusion in the Nile Delta aquifer**

Egypt. Hydrogeol. J., s464–465 (20) (2012), pp. 186-198

Solomon et al., 2007

S. Solomon, D. Qin, M. Manning, *et al.***Climate change 2007: The physical science basis. Contribution of working group I to the fourth assessment report of the Intergovernmental Panel on Climate Change**

Comput. Geom., 18 (2) (2007), pp. 95-123

Voss and Provost, 2002

C.I. Voss, A.M. Provost**SUTRA, a model for saturated–unsaturated variable density ground-water flow with energy or solute transport**

US Geol. Surv., 2 (2002), p. 4231

Wang et al., 1995

D.C. Wang, R.Q. Zhang, Y.H. Shi, *et al.***Hydrogeology fundamentals**

Geological Publishing House (1995)

Wang et al., 2003

Z.Y. Wang, G.L. Meng, S.Q. Wang**Geochemistry modeling of quaternary subsurface brines in south coast of the Laizhou Bay, the Bohai sea**

Mar. Geol. Quat. Geol., 23 (1) (2003), pp. 49-53

Werner and Gallagher, 2006

A.D. Werner, M.R. Gallagher**Characterization of sea-water intrusion in the Pioneer Valley, Australia using hydrochemistry and three dimensional numerical modelling**

Hydrogeol. J., 14 (8) (2006), pp. 1452-1469

Werner et al., 2013

A.D. Werner, M. Bakker, V.E.A. Post, A. Vandenbohede, C.H. Lu, B. Ataie-Ashtianiab, C.T.Simmonsab, D.A. Barry**Seawater intrusion processes, investigation and management: recent advances and future challenges**

Adv. Water Resour., 51 (1) (2013), pp. 3-26

Wu et al., 1993

J.C. Wu, P.M. Liu, Q.B. Jiang, J.J. Wang**Seawater intrusion in Laizhou Bay district of Shandong Province**

Geol. Jiangsu, 17 (1) (1993), pp. 27-31

Xu and Hu, 2017

Z. Xu, B.X. Hu**Development of a discrete-continuum VDFST-CFP numerical model for simulating seawater intrusion to a coastal karst aquifer with a conduit system**

Water Resour. Res., 52 (2017), 10.1002/2016WR018758

Xu et al., 2016

Z. Xu, S. Bassett, B.X. Hu, S. Dyer**Long-distance seawater intrusion through karst conduit networks in the Woodville Karst Plain with the attraction of Wakulla Springs**

Sci. Rep. (2016), 10.1038/srep32235

Xu et al., 2018

Z. Xu, B. Hu, X. Hu, M. Ye**Numerical modeling and sensitivity analysis of seawater intrusion in a heterogeneous coastal karst aquifer with conduits**

Hydrol. Earth Syst. Sci., 22 (2018), pp. 1-19

Xue et al., 1997

Y.Q. Xue, J.C. Wu, C.H. Xie, Y.X. Zhang**Research of seawater and salt water intrusion of Laizhou Bay**

Chin. Sci. Bull., 11 (22) (1997), pp. 2360-2368

Yang et al., 2013

J. Yang, T. Graf, M. Herold, T. Ptak**Modeling the effect soft tide sandstorm surges on coastal aquifers using a coupled surface-subsurface approach**

J. Contam. Hydrol., 149 (6) (2013), pp. 61-75

Yechieli et al., 2001

Y. Yechieli, U. Kafri, M. Goldman, C. Voss**Factors controlling the configuration of the fresh-saline water interface in the Dead Sea coastal aquifers: synthesis of TDEM surveys and numerical groundwater modeling**

Hydrogeol. J., 9 (4) (2001), pp. 367-377

Zhang et al., 1997

Y.X. Zhang, Y.Q. Xue, H.H. Chen**Chemical composition variation in groundwater caused by salt-brine water intrusion and its affection to environment in Weifang area**

Acta Sceent. Circumstanti., 17 (3) (1997), pp. 295-301

Zhang et al., 1999

Y. Zhang, Y.Q. Xue, C.H. Xie, J.C. Wu**The motion equation of high concentration situation**

J. Naijing Univ., 35 (3) (1999), pp. 309-315

Zhang et al., 2017

X.Y. Zhang, J.J. Miao, X.H. Bill, H.W. Liu, H.X. Zhang, Z. Ma**Hydrogeochemical characterization and groundwater quality assessment in intruded coastal brine aquifers (Laizhou Bay, China)**

Environ. Sci. Pollut. Res., 2 (2017), pp. 1-18